Effect of climate change on slope stability. A numerical analysis using predictions of the Catalan Pyrenees

Stephania Rodríguez, Carol Puig-Polo, Antonio Lloret, Jean Vaunat, Marcel Hürlimann

Universitat Politècnica de Catalunya (UPC)

stephania.rodriguez@estudiant.upc.edu

Abstract

The effect of climate change on soil loss processes in mountainous areas represents a current and critical problem. In this work, this issue is addressed through the analysis of the stability of different types of slopes subjected to climatic actions by 1D thermo-hydraulic numerical modeling and the infinite slope approach. The study aims to establish an average value of the safety factor, its variance and the probability of failure for the conditioning factors.

The atmospheric values incorporated in the stability calculations are from regional climate change predictive models. The correlation data considers the most appropriate climate change projection for our study area located in the Central Pyrenees (Spain). Current reports, when considering the Mediterranean area, predict a rise in temperature up to 4.8 ° C for the largest projections of greenhouse gas emissions, which influence thermal flux and heat transfer patterns and mass storage processes, hydraulic conductivity values, changes in saturation degrees and liquid pressures. While the rainfall in the winter season decreases, the intensity and duration remain through all stability analysis as one of the parameters with the greatest influence of all climatic factors, by directly intervening in the increase in pore fluid pressures.

The application of an infinite slope model for the analysis of the safety factor allows a stability analysis when evaluating the responses of the numerical model Code Bright. Code Bright incorporates the problem of flow and balance of water, air and energy, and the reaction to atmospheric scenarios for different soil types and the thermal and hydraulic properties that influence the development of the slope failure. The evolution of the safety factors related to the atmospheric variables describes the components of the instability and the sensitivity of the constitutive parameters of the soil. Other factors such as heterogeneous resistances within the coupled model allow us to describe a more characteristic state of natural slopes.

The results show that the greatest impacts arise in years under climatic indices of high temperatures or above the averages of their categories. Precipitation values remain in average ranges, but the year precedent rainfall having a statistically higher mean value. On average these episodes of failure are estimated for rainfall between 40 and 60 mm, with higher probability for extreme rainfall of 90 mm. The period 2041-2070 illustrates an increase in instability events and a decrease in return periods for the three types of soils considered in the numerical modeling.

1 INTRODUCTION

Landslides are one of the geological - geotechnical phenomena with greatest impact in human communities. When considering the soil-vegetation-atmosphere interactions, we must consider the influence of climate change as one of the current components with the greatest impact on the treatment of slope stability analysis. The governing factor of the slope failures are the sum of all the interactions of the geotechnical parameters and the atmospheric components, which leads to a more regional focus on climate change projections for the study area of the Catalan Pyrenees for 1961 – 2100.

Climate change and slope stability factors consider the following states: average annual temperature, intensity and duration in annual rainfall, evapotranspiration and soil temperature. Changes in these factors create the possibility of major landslides, for the same geometrical and geomechanical conditions. These atmospheric aspects are incorporated in a numerical model in response to rainfall and temperature (which mainly controls evapotranspiration), using a unidimensional column and daily time steps.

The main objective is to perform a slope stability analysis using the numerical model Code Bright, when considering the effects of atmospheric processes of predictive climatic models for the study area. That would lead to a localized analysis of changes in the safety factor patterns of a few type slopes.

1.1 Climate Change Projections

Entities such as the Intergovernmental Panel on Climate Change (IPCC) and the European Environment Agency (EEA) collect information for the assessment and modeling of the phenomena related to climate change. Global IPCC climate change reports describe a temperature increase of 0.3-1.7°C for the lower emission scenarios, and 2.6-4.8°C for higher emissions.

Reports also show that temperature changes between 1976 and 2006 increase from 0.2 to 2°C per decade (EEA, 2017) in the entire European region. In addition, there have been increases in the intensity and frequency of intense precipitation between 2002-2011, while the temperature has suffered an increase above pre-industrial levels by 1.3°C (Tang et al., 2018). When evaluating both global and regional climate change models, the European Mediterranean area presents a temperature increase greater than the European average and the annual rainfall will be lower (Kelemen et al., 2009).

1.2 Regional Climate Context

In 2006, the Government of Spain published the National Climate Change Adaptation Plan with the objective of studying the evolution and impacts of climate change in the Spanish territory. It particularly assigned to the State Meteorological Agency (AEMET) the mandate to develop models based on dynamic and statistical methodologies, taking as reference the already established global prediction models (Francés et al., 2017).

The maximum temperature values of the historical period of 1961 - 2000 express a linear growth of 0.89 % for the winter season, while the evolution of the summer season shows a 2.21 % evolution. When comparing these values with the period of 2011-2100, the trends grow significantly by 7.54 % for the summer and, 4.52 % for the winter.

The years between 2020 and 2060 are the projections closest to the estimates of the IPCC reports, with an increase of 5° C. In turn, the first years of the analysis show the highest minimum temperature indices, which lowers the threshold of heat influence within the studied area.

As for annual rainfall, general predictions within the regional context lead to consider decreases in the winter seasons with greater impact of extreme rainfall. Models foresee an average loss of 200 mm of rainfall for 2011 - 2100 compared to the historical data. An increase in variability in the period comprised between 2011 and 2100 indicates a higher probability of obtaining consecutive percentiles less than 10% (warm years) and greater than 90% (wet years) in the time series.

1.3 Landslide analysis

Different studies have focused on the analysis of the influence of different climate factors on the occurrence of landslides. Authors such as Buma and Dehn, (1998), Collison et al., (2000) and Gariano et al., (2017) have established regional benchmarks for evaluating the temporary stability trends for climate change scenarios, local hydrological studies, and geomorphological models. Alvioli et al., (2018) emphasized the effect of duration and intensity of rainfall as an intensifying factor of failures.

Collison et al., (2000) conducted studies for England in a 4km zone, where the estimated geographic and hydrological information shows an increase in rainfall that will be equal to evapotranspiration, which keeps the number of failure events stable.

This study aims at presenting a preliminary assessment of the effect of climate change on shallow landslides in the Catalan Pyreneans.

2 DATA AND METHODS

The methodology considered in this work consists in assessing the long-term evolution of the Safety Factor of an infinite slope subjected to climate changes predicted by regional models. As a first sept, time evolutions of water pressures will be calculated in a vertical column of soil using a finite element program purposely developed to include the application of climatic variables. Afterwards, water pressures output by the numerical model will be used to calculate the change with time of slope Safety Factor.

2.1 Climate change modeling

The present analysis is based on climatic data outcoming from the General Circulation Model (GCM) ECHAM5, the RCA3 regional model and the RCP 8.5 (Representative Concentration Pathways); for a 20 x 20 km area (0.75 E; 42.5 N).

The GCM can be defined as a three-dimensional representation of the interactions between meteorological, hydrological and climate parameters on a worldwide scale.

Areas with complex topographies and wide contrasts of the most relevant climatic parameters need to include regional climate models to reduce the study area, obtain a better resolution for extreme weather events and introduce seasonal and daily variables in the European region (Samuelsson et al., 2011).

The coupling between global, regional models and emission scenarios allows to carry out dynamic regionalization of climatic projections and to represent the interactions of variables through a consistent set of parameters, namely precipitation, maximum and minimum daily temperature, evaporation, wind speed, relative humidity and radiation.

2.2 Correlation to observational data

According to Chow et al., (1988), the estimation of rainfall on delimited regions requires a wide data coverage of intensity and duration of precipitation that must be representative of the study area. As well, the available sources of historical atmospheric information must be compatible with climate change prediction models.

The reanalysis Spain02, developed by the University of Cantabria and the Spanish Meteorological Agency (AEMET), reports historical climatic values of Spain (Turco et al., 2017). It provides precipitation and temperature data with a resolution of 0.2° and based on records of 2756 stations from 1950 to 2008 (Herrera et al., 2010). It has been used in downscaling studies carried out by comparing the main values of the precipitation indices to regional climate change models.

Between them, RCA3 model shows one of the minor deviations from the observational data. General trends indicate that precipitation are the parameters exhibiting less correlation within the global models, due to the complexity of the water cycles. Conversely, the collected maximum temperatures exhibit less variability across the different studies and appear to depend directly on the emissions scenario.

2.3 Thermohydraulic modeling in Code Bright

For the computation of water pressures in the infinite slope, a Finite Element model has been run using the code Code Bright. The latter performs coupled mechanical, hydraulic and thermal analyzes (Olivella et al., 1994). Pre- and post-processing are executed through the GiD platform of the International Center for Numerical Methods in Engineering, (CIMNE, 2020).

The Finite Element formulation generally resolves the equations of water mass (including liquid water and vapour), air mass and energy balance to assess changes of soil thermal and hydraulic states with time. Methods adopted for the resolution of the system of nonlinear partial differential equations are described in Olivella et al., (1994). In this specific study, air mass balance has been deactivated and the air pressure is considered constant and equal to 100 kPa in all the analyses.

The numerical formulation includes moreover a boundary conditions to simulate evaporation, precipitation, radiation, and convective and advective energy flows.

2.3.1 Geometry and General data

The geometry considered for the model is an one-dimensional column of 50 m height, with a water table at 5 m below the surface. Three types soil have been studied: poorly graded sand, silt, and clay.

2.3.2 Initial and Boundary conditions

Prescription of boundary and initial conditions requires the definition of parameters for water and energy as well as climatic time series.

- Initial state

It is defined by initial profiles of temperature and water pressure. A constant temperature is set along the column. Distribution of water pressure is considered hydrostatic below and above the water table.

Table 1. Atmospheric parameters of the study area

Latitude, radians	0.73958
Fall start time, s	2,29824 10^7
Time at noon, s	43200
Rough Length, m	0.2
Screen height, m	2.0
Stability factor, kg / m^3	1.0
Atmospheric gas density, kg / m^3	1,225
Dried albedo	0.15
Wet albedo	0.10
Gas gamma, kg/ m^2 / s / MPa	10^6
Liquid gamma, kg/m^2 / s / MPa	-10^6
Precipitation multiplier factor	1.0
Radiation multiplier factor	1.0
Evaporation multiplier factor	1.0
Type of radiation	3.0
Vegetation fraction	0

Table 2. Atmospheric data

Data	Units
Atmospheric temperature, T_a	° C
Atmospheric gas pressure, P_{ga}	MPa
Relative Humidity, H_r	-
Radiation, R_n	J/m^2s
Cloud index, I_n	-
Precipitation, P	kg/ m^2s
Wind speed, v_a	m / s

- Initial porosity

Different values of initial porosity have been assigned according to material type. This parameter plays a significant role as it modifies values of thermal conductivity, water and gas storage coefficients, diffusion coefficient and hydraulic conductivity.

- Contour flow conditions

Temperature and water pressure have been fixed at a constant value (equal to the initial value) at the bottom of the column.

The condition at the surface of the column is prescribed as a time series of solar radiation, precipitation, air temperature, air relative humidity and wind velocity outcoming from the model of climate change up to year 2100. The condition requires moreover the definition of several soil-atmosphere interaction parameters (see Table 1 and Table 2) in order to include effects of solar radiation incidence (related to time and latitude), solar radiation reflection (related to soil albedo) and wind profile (related to surface roughness, height of wind measurement and air mass stability). Note that the precipitation input in the model is directly the net precipitation (total precipitation minus run-off).

2.4 Thermo-hydraulic modeling

Following Alonso et al., (1992) and Alonso et al., (1995), three characteristic soil types have been chosen: a poorly graded silty sand, a silt and a clay. In order to solve the water mass and energy balance equations in terms of liquid pressure (P_l) and temperature (T), it is necessary to consider relationships and parameters that define the thermohydraulic behavior of the soil in partially saturated conditions (Olivella et al., 2019)

- Retention curve

The van Genuchten relationship (van Genuchten, 1980) has been adopted (equation 1). Table 3 shows the associated parameters for the three types of soil considered (according to Alonso et al., 1992).

$$S_e = \frac{S_l - S_{rl}}{S_{ls} - S_{rl}} = \left(1 + \left(\frac{P_g - P_l}{P}\right)^{\frac{1}{1-\lambda}}\right)^{-\lambda} \tag{1}$$

$$P = P_0 \; \frac{\sigma(T)}{\sigma_0}$$

S_l and Se are the saturation degree and the effective saturation degree of the liquid phase. σ_0 is the surface tension at temperature in which P_0 was measured.

Table 3. Parameters used for the retention curve

	Sand	Silt	Clay
P_0(MPa)	0.01	0.10	1.00
σ_0 (N/m)	0.072	0.072	0.072
λ	0.872	0.405	0.107
S_{rl}	0.02	0.20	0.30
S_{ls}	1.00	1.00	1.00

- Intrinsic permeability

Values of permeability are taken from Alonso et al., (1992) and Chow et al., (1988). Since calculations do not include mechanical aspects, possible variations in permeability due to changes in soil porosity have not been considered.

Table 4. Intrinsic Permeability Parameters

	Sand	Silt	Clay
k (m^2)	10^{-12}	10^{-14}	10^{-16}

- Relative permeability for the liquid phase

It is affected by changes in degree of saturation, which is linked to suction values through the van Genuchten relationship (van Genuchten, 1980). In this study, the dependency proposed in Equation (2) has been adopted. Parameters are indicated in Table 3.

$$k_{rl} = \sqrt{S_e}\left(1 - \left(1 - S_e^{1/\lambda}\right)^{\lambda}\right)^2 \quad (2)$$

- Diffusive vapor flow in gas phase

It follows Fick's law using a molecular diffusion coefficient D_g^w(m^2/s) dependent on temperature (equation 3). Parameter n and D are taken equal to 2.3 and 5.9 10-6 Pa m^2/s K^{-n}, respectively.

$$D_g^w = D\left(\frac{(273.15 + T)^n}{P_g}\right) \quad (3)$$

- Heat conductive flow

It is modeled by Fourier's law using a thermal conductivity (λ) that depends on the liquid degree of saturation (see equation 4). Values of dry and saturated thermal conductivity are indicated in Table 5. They have been taken from Ghanbarian & Daigle (2016).

$$\lambda = \lambda_{sat}\sqrt{S_l} + \lambda_{dry}\,(1 - \sqrt{S_l}\,) \quad (4)$$

Table 5. Parameters of Heat Conductive Flow

	Sand	Silt	Clay
λ_{dry} (W/(Km))	0.253	0.225	0.222
λ_{sat} (W/(Km))	2.186	1.401	1.367

2.5 Safety Factor

The infinite slope theory is used for the analysis of safety factors. It takes as input the water pressures previously obtained by the thermo-hydraulic model. Safety factor (SF) is calculated through equation 6 (see also Figure 1). Parameters includes soil specific weight (γ), cohesion (c) and friction angle (ϕ). The effect of suction on the shear strength is considered by an increment of normal stress equal to suction multiply by the effective degree of saturation (Alonso et al., 2013), see equation (5). Note that in saturated state expression (5) becomes the classic expression of shear strength in terms of effective stresses.

Table 6. Safety factor analysis parameters

	Sand	Silt	Clay
S_{ls}, Maximum saturation	1.00	1.00	1.00
S_{rl}, Residual Saturation	0.02	0.20	0.30
c', (kPa), Effective cohesion	0	0	4
γ, (kN / m^3), Specific weight	20	20	20
φ, (°), Friction angle	35	25	25
β, (°), Slope angle	45	45	45

$$\tau = c' + \sigma_n \tan\phi + (P_g - P_l)\,S_e \tan\phi_b \quad (5)$$

$$SF = \frac{c}{\gamma H \cos\beta \sin\beta} + \frac{\tan\phi}{\tan\beta} + \frac{(P_g - P_l)S_e \tan\phi}{\gamma H \cos\beta \sin\beta} \quad (6)$$

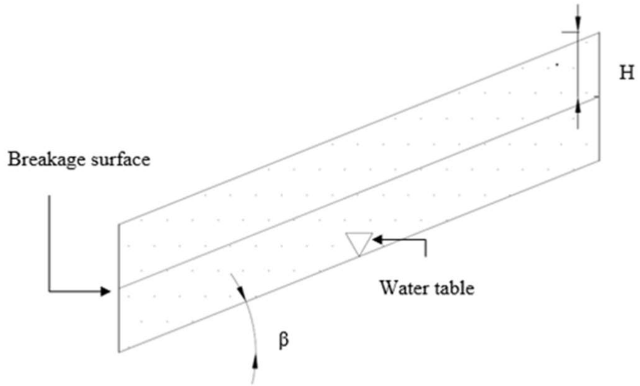

Figure 1. Slope geometry considered in the infinite slope approach. H is the failure depth, γ the soil specific weight, β the slope angle.

3 RESULTS

Time evolutions of water pressures and Safety Factors are presented for the three types of soils.

3.1 Clay

Fig. 2 shows the time evolution of suction (difference between air pressure – considered constant – and water pressure) obtained in the case of the clay material. For the 2011-2100 period, suction values close to the surface reach minima and maxima between 100 and 600 kPa (Figure 2), while mean values exhibit a linear positive trend of about 5 kPa by year. This is consistent with the prediction of an increase in temperature during the same period, which is expected to enhance evapotranspiration in the soil. This effect appears to be more important during the last 50 years of the period, when suction cycle amplitude and suction mean value are higher than in the first 40 years.

Values of suctions at depth exhibit lower variations with time, because of cycle attenuation resulting from the delayed process of water movement towards the evaporative boundary. However, mean values at 3 and 5 m remain close to the ones at soil surface (around 350 kPa) and have a similar rate of increase with the years. This aspect is related to the shape of the retention curve for clay material, which presents low variations of water content for the range of suction prevailing in the soil (between 100 and 600 kPa).

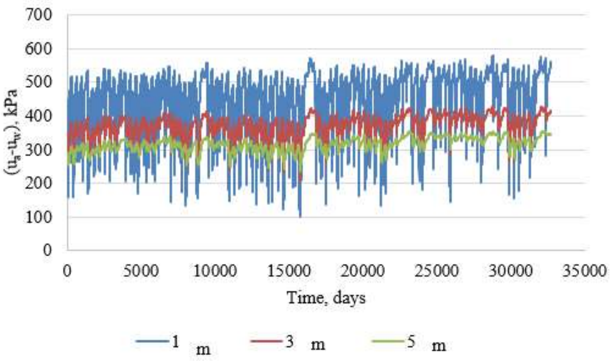

Figure 2. Suction at different depths of the clay column (2011-2100)

3.2 Silt

Fig. 3 shows the time evolution of suction for the case of the silt material. Values range between 30 kPa at 5 m (corresponding to a saturation close to 1) and 120 kPa on surface (corresponding to saturation around 0.75). Such distributions highlight the predominance of quite low suctions in the layer, which is prejudicial for the stability of the slope. Moreover, large drops of suction can be identifiable from time to time as the result of the occurrence of extreme rainfall events, which let expect the reach of marginal stability or even failure. It is interesting to note that, although the mean value of suction slightly increases with time (indicating a tendency to move towards drier slopes during the century), the effect of extreme events remain essentially the same at the beginning and end of the century.

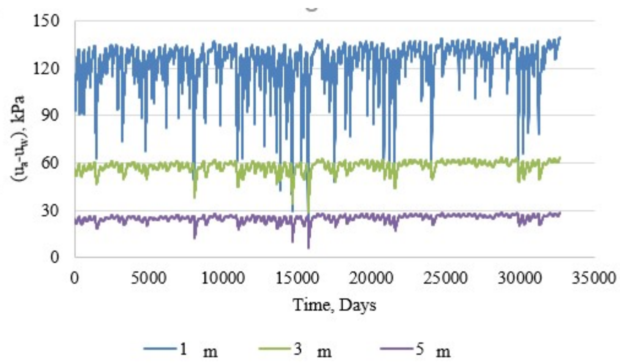

Figure 3. Suction at different depths of the silt column (2011-2100)

3.3 Sand

Fig. 4 shows the time evolution of suction in the sand column. In this permeable material with low capillary ascent, rainfall penetrates quickly at depth, while evaporation is limited by the presence of an upper vadose zone at residual water content. This leads to a high-water table, located around 2m depth, and low suctions in the unsaturated layer. A slight drawdown of the water table seems to occur during the century, without exceeding some tenths of centimeters.

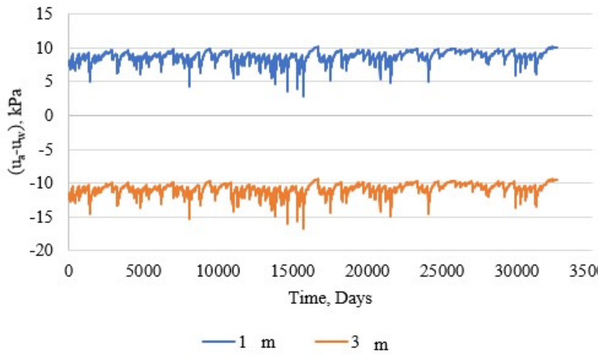

Figure 4. Suction at different depths of the sand column (2011-2100)

3.4 Safety Factor

Figure 5 depicts the number of failure events predicted by the infinite slope model for the case of the clay column. They correspond to times when the Safety Factor becomes equal to 1.

From a general point of view, the model predicts a significant higher number of events over the whole period. It indicates moreover a high landslide activity during the period 2011 – 2040, which is consistent with the low values of temperature indices predicted by the regional model of climate change. Low temperatures are indeed accompanied by reduced evaporation and higher pore pressure inside the slope.

Conversely, the period 2071 – 2100 is characterized a few landslides events, because predicted temperatures are greater than in the previous period and annual rainfall lower. As a result, higher suctions prevail in the slope, increasing their stability.

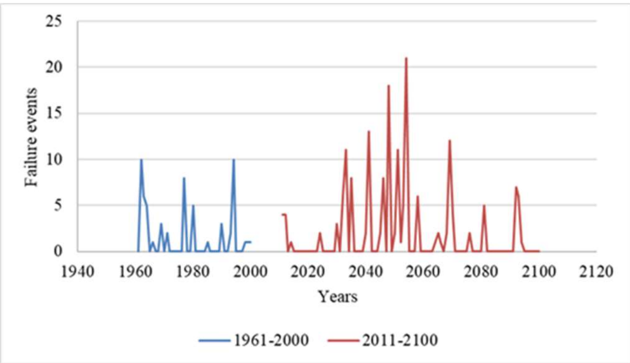

Figure 5. Number of failure events for the clay column (historic and predictive models)

3.5 Climate context

Models allow moreover having an insight into the relationship between failure occurrence and daily accumulated rainfall. According to the prediction, failures in years having several events close to the average number of the 2011-2100 period take place for precipitation values between 40 and 60 mm. The additional failures occurring in years with maximum number of events occurs for daily accumulated rainfall above 90 mm.

Another aspect relies on the climatic characteristics of the years with highest number of failures: 1994 for the test period (1961-2000) and 2054 for the simulation period (2011-2100). On the one hand, they are both provided with maximum temperature values and frost indexes, which indicates very warm years in their respective periods. On the other hand, in both cases, rainfalls values are within a normal range, but the year before exhibits high precipitation indices. This fact illustrates the importance of antecedent rainfall and hydraulic state at time of occurrence of the triggering rainfall event and the necessity to run long time numerical simulation for any suitable analysis of slope stability under climatic actions.

4 CONCLUSIONS

The period 2041-2070 illustrates an increase in failure events and a decrease in return periods for the three types of soils. Conditioning the climate change parameters of the study area to risk points for the projections and emission scenarios of this time series.

The presence of a stable number of extreme rainfall events, in the second analysis period, despite the decrease in annual rainfall, describes a higher intensity for the time and zone affected, which is an important factor within the slope stability studies.

In the cases of slope stability analysis, geometric conditions and thermohydraulic parameters when modeled in combination with climatic components such as extreme precipitation events, establish equilibrium states and failure points within the study of safety factors. The slope responds to the climatic factors through high suction points of up to 600 kPa in clays, and the development of interstitial pressures in the sands.

The permeability and retention curves being the variables with the greatest impact of the level of rainfall affectation. The intensity and duration of precipitation remain through the entire stability analysis as the most important parameters, by directly intervening in the increase in pore fluid pressures.

Another important factor to include is the temperature, which affects the thermal flux and heat transfer patterns and mass storage processes, hydraulic conductivity values, changes in saturation degrees and pressures liquids, which creates alterations in water flow processes.

The patterns of the safety factor of the type of soil allow us to understand the changes in the number of estimated failure events on an annual scale and the triggers. It illustrates the effect of the values of the suction in the stabilization of the land, and the relation with the changes of temperature, this in relation mainly with the clay and smaller measurement with silt.

The processes with the greatest impact coming from years under climatic indices of high temperatures. At the same time, precipitation values describe wet years but being the precedent rainfall factor a vital parameter in the transition to interstitial pressure failures.

On average these episodes of failures are estimated for rainfall between 40 and 60 mm, with large movements in events of extreme rainfall of 90 mm, which is common for the storage capacity of the land.

5 ACKNOWLEDGMENTS

We thank the entire team of the SMuCPhy project and its funding by the Spain Government (BIA 2015-67500-R) and AEI/FEDER, UE, and supported partially by the SENACYT Foundation – Panama.

6 REFERENCES

Alonso, E. E., García Merino, J. V., & Lloret, A. (1992). Efecto de la infiltración de agua en la estabilidad de taludes de suelos parcialmente saturados. *III Simposio Nacional Sobre Taludes y Laderas Inestables*, *1976*, 387–398.

Alonso, E. E., Gens, A., Lloret, A., & Delahaye, C. (1995). Effect of rain infiltration on the stability of slopes. *Proceedings of the First International Conference on Unsaturated Soils Volume 1*, 241–249.

Alvioli, M., Melillo, M., Guzzetti, F., Rossi, M., Palazzi, E., von Hardenberg, J., Brunetti, M. T., & Peruccacci, S. (2018). Implications of climate change on landslide hazard in Central Italy. *Science of the Total Environment*, *630*, 1528–1543. https://doi.org/10.1016/j.scitotenv.2018.02.315

Buma, J., & Dehn, M. (1998). A method for predicting the impact of climate change on slope stability. *Environmental Geology*, *35*(2–3), 190–196. https://doi.org/10.1007/s002540050305

Chow, V. Te, Maidment, D. R., & Mays, L. W. (1988). *Applied Hydrology* (Internatio). McGraw Hill.

CIMNE. (2020). *GiD v14*. https://www.gidhome.com/

Collison, A., Wade, S., Gri, J., & Dehn, M. (2000). *Modelling the impact of predicted climate change on landslide frequency and magnitude in SE England*. *55*, 205–218.

EEA. (2017). *Climate change, impacts and vulnerability in Europe 2016* (Issue 1).

Francés, P. A., Calle, M. J. C., Saavedra, A. P., Calzado, P. R., & Camino, E. R. (2017). *Guía de escenarios regionalizados de cambio climático sobre España a partir de los resultados del IPCC-AR5*.

Gariano, S. L., Rianna, G., Petrucci, O., & Guzzetti, F. (2017). Assessing future changes in the occurrence of rainfall-induced landslides at a regional scale. *Science of the Total Environment*, *596–597*, 417–426. https://doi.org/10.1016/j.scitotenv.2017.03.103

Ghanbarian, B., & Daigle, H. (2016). Thermal conductivity in porous media: Percolation-based effective-medium approximation. *Water Resour. Res.*, *52*, 295–314. https://doi.org/10.1002/2015WR017236.Received

Herrera, S., Ancell, R., & Pons, M. R. (2010). *Development and analysis of a 50-year high-resolution daily gridded precipitation dataset over Spain (Spain02)*. 1–19. https://doi.org/10.1002/joc.2256

Kelemen, A., Munch, W., Poelman, H., Gakova, Z., Dijkstra, L., & Torighelli, B. (2009). Regions 2020: The climate change challenge for european regions. *European Commission*, *March*, 27. https://doi.org/10.1016/j.nucengdes.2011.01.052

Olivella, S., Carrera, J., Gens, A., & Alonso, E. E. (1994). Nonisothermal multiphase flow of brine and gas through saline media. *Transport in Porous Media*, *15*(3), 271–293. https://doi.org/10.1007/BF00613282

Olivella, S., Vaunat, J., & Rodríguez-Dono, A. (2019). *Code Bright User's Guide* (Universitat Politècnica de Catalunya (UPC) (ed.); Version 9, Issue May). Department of Civil and Environmental Engineering.

Samuelsson, P., Jones, C. G., Willén, U., Ullerstig, A., Gollvik, S., Hansson, U., Jansson, C., Kjellström, E., Nikulin, G., & Wyser, K. (2011). The Rossby Centre Regional Climate model RCA3: Model description and performance. *Tellus, Series A: Dynamic Meteorology and Oceanography*, *63*(1), 4–23. https://doi.org/10.1111/j.1600-0870.2010.00478.x

Tang, A. M., Hughes, P. N., Dijkstra, T. A., Askarinejad, A., Brenčič, M., Cui, Y. J., Diez, J. J., Firgi, T., Gajewska, B., Gentile, F., Grossi, G., Jommi, C., Kehagia, F., Koda, E., ter Maat, H. W., Lenart, S., Lourenco, S., Oliveira, M., Osinski, P., … Van Beek, V. (2018). Atmosphere–vegetation–soil interactions in a climate change context; impact of changing conditions on engineered transport infrastructure slopes in Europe. *Quarterly Journal of Engineering Geology and Hydrogeology*. http://qjegh.lyellcollection.org/content/early/2018/03/20/qjegh2017-103.abstract

Turco, M., Llasat, M. C., Herrera, S., & Guti, J. M. (2017). Bias Correction and Downscaling of future RCM Precipitation Projections using a MOS-Analog Technique. *American Geophysical Union*. https://doi.org/10.1002/2016JD025724

van Genuchten, M. T. (1980). A Closed-form Equation for Predciting the Hydraulic Conductivity of Unsaturated Soils. *Soil Sci. Soc. Am. J.*, *44*, 892–898.